Journal of Alloys and Compounds 509 (2011) 217–220

Contents lists available at ScienceDirect

Journal of Alloys and Compounds

journal homepage: www.elsevier.com/locate/jallcom

Specific heat of the antiferro/ferro-magnet $NpGa_3$

E. Colineau*, J.-C. Griveau, F. Wastin, J. Rebizant

European Commission, Joint Research Centre, Institute for Transuranium Elements, Postfach 2340, 76125 Karlsruhe, Germany

ARTICLE INFO

Article history:
Received 17 August 2010
Received in revised form
14 September 2010
Accepted 19 September 2010
Available online 25 September 2010

Keywords:
Actinide alloys and compounds
Magnetically ordered materials
Heat capacity
Phase diagrams
Phase transitions

ABSTRACT

The specific heat of $NpGa_3$ has been measured for the first time. The magnetic transitions and more generally the full magnetic phase diagram have been re-established precisely. The Sommerfeld coefficient and the magnetic entropy point to a rather localized system, in agreement with previous studies, in particular high pressure Mössbauer and resistivity. The comparison with other NpX_3 suggests that $NpGa_3$ is the most localized member of the series.

1. Introduction

The actinide compounds AnX_3 (An = U, Np, Pu), where X is an element from Group IIIA or IVA, mostly crystallize into the cubic $AuCu_3$ structure. They are characterized by an actinide–actinide interatomic distance far above the Hill limit, therefore *5f*–ligand hybridization is the main mechanism responsible for the delocalization of the *5f* electrons. The systematic of this hybridization has been well demonstrated for the UX_3 compounds, which either do not order magnetically (X = Al, Si, Ge, Sn) or exhibit antiferromagnetism (X = Ga, In, Tl, Pb). It was concluded that the *5f*–ligand hybridization increases as one moves up a column of the periodic table or moves from a Group IIIA element to a Group IVA element [1,2].

Although data on corresponding Np intermetallics are much less documented, a similar trend was noticed. However, it is clear that the Np-based compounds are more "magnetic" than their uranium analogues, which is consistent with the general picture that the hybridization decreases as one substitutes a heavier actinide. Indeed, all NpX_3 compounds (X = Al, Ga, In, Sn) order magnetically at the exception of $NpGe_3$ and $NpSi_3$ [3–5]. In the plutonium series, magnetic order was observed only in $PuGa_3$ [6], whereas $PuIn_3$ [7] and $PuSn_3$ [8] are paramagnets. $PuAl_3$, $PuGe_3$, $PuTl_3$ and $PuPb_3$ have been reported, but their physical properties are not known [9]. It is worth noting that several PuX_3 (X = Al, Ga, Tl) crystallize into non-cubic structures.

The AnX_3 (An = U, Np, Pu) series, with its generally simple crystallographic structure and rich magnetic and electronic properties, allows a systematic study of the dual character of the *5f* electrons. The knowledge of specific heat behavior at low temperature is an important aspect to understand these systems. Several UX_3 systems (X = Al, Ga, In, Sn, Pb) present enhanced specific heat at low temperature, in particular USn_3 ($\gamma = 170\ mJ\ mol^{-1}\ K^{-2}$) and UPb_3 ($\gamma = 110\ mJ\ mol^{-1}\ K^{-2}$). The highest value was found in $PuGa_3$ where the values of the electronic specific heat coefficient γ amounts to ~110 and ~220 $mJ\ mol^{-1}\ K^2$ for the trigonal and hexagonal allotropes, respectively [6]. In the neptunium analogues, only $NpSn_3$ ($\gamma = 88\ mJ\ mol^{-1}\ K^{-2}$) [10], $NpIn_3$ ($\gamma = 72\ mJ\ mol^{-1}\ K^{-2}$) [11] and $NpGe_3$ ($\gamma = 34\ mJ\ mol^{-1}\ K^{-2}$) [12] have been investigated so far.

$NpGa_3$ exhibits antiferromagnetic ordering ($k = (1/2\ 1/2\ 1/2)$) below $T_N \approx 65$ K, but ferromagnetic order with an ordered moment $\mu_{Np} \approx 1.5\mu_B$ is stabilized below $T_C \approx 50$ K [3,13,14]. The high pressure behavior of $NpGa_3$ suggests a rather localized character of the *5f* electrons [15]. We report here for the first time the specific heat properties of $NpGa_3$.

2. Experimental

The $NpGa_3$ sample was prepared by arc melting of stoichiometric amounts of neptunium and gallium metal in dry argon gas. X-ray-diffraction patterns obtained with a Debye–Scherrer camera showed a pure cubic $AuCu_3$ phase (space group *Pm*3*m*) with a lattice parameter $a = 4.255$ Å. The specific heat experiments were performed using a 14.171 mg $NpGa_3$ polycrystalline sample by the relaxation method in a Quantum Design PPMS-14 within the temperature range 1.8–300 K and in magnetic fields up to 14 T.

* Corresponding author. Tel.: +49 0 7247 951 442; fax: +49 0 7247 951 599.
E-mail addresses: eric.colineau@ec.europa.eu, ecolineau@ec.europa.eu (E. Colineau).

0925-8388/$ – see front matter © 2010 Elsevier B.V. All rights reserved.
doi:10.1016/j.jallcom.2010.09.109

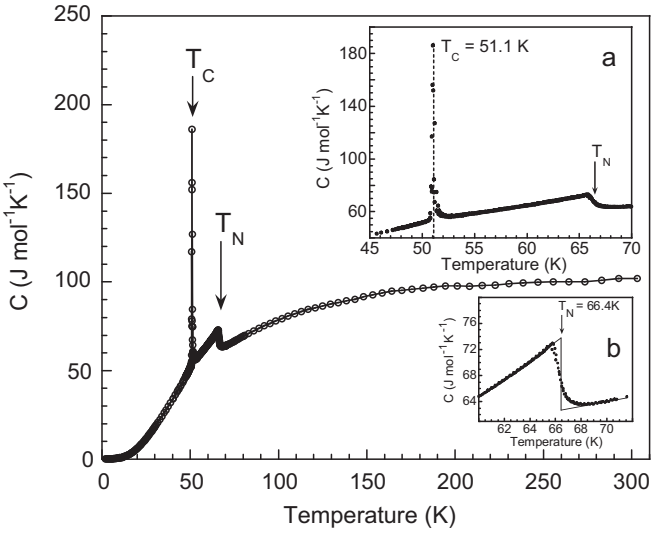

Fig. 1. Specific heat of $NpGa_3$ as a function of temperature. The inset 'a' shows a closer view of the magnetic transitions. Inset 'b' shows an entropy-conserving construction to determine precisely the Néel temperature.

3. Results

Fig. 1 shows the temperature dependence of the specific heat in $NpGa_3$ over the whole temperature range investigated. The room-temperature value ($C \approx 100\,\mathrm{J\,mol^{-1}\,K^{-2}}$) corresponds to the Dulong–Petit limit, as expected for a heavy intermetallic system where 6 degrees of freedom are available for each of the 4 atoms:

$$C = 4 \times 6 \times \frac{k_B N_A}{2} \quad (1)$$

with k_B the Boltzmann constant and N_A the Avogadro number.

When the temperature decreases, we observe two anomalies (inset Fig. 1). First, a lambda-type anomaly occurs at 66.5 K that corresponds to the onset of antiferromagnetic ordering established by previous studies [13]. The Néel temperature can be precisely determined using an entropy conserving construction (inset b). At 51.1 K, a remarkably intense and narrow peak emerges from the curve, indicating the magnetic phase transition from antiferromagnetism to ferromagnetism. This sharp peak confirms the first-order nature of the transition, as previously revealed by the thermal variation of the magnetic moment measured by Mössbauer spectroscopy and neutron diffraction [13].

The application of an external magnetic field affects both transitions in different ways (Fig. 2): the Néel temperature is slightly shifted to lower temperature, before the antiferromagnetic order is destroyed above 4 T. On the contrary, the peak corresponding to the antiferromagnetic/ferromagnetic transition is largely shifted to higher temperatures, until it meets and absorbs the lambda-type anomaly. The topology of the peak evolves from a first-order like, sharp peak to a second-order like transition through a possible tricritical point.

From these observations, we can reconstruct the magnetic phase diagram of $NpGa_3$, which is in agreement with the previously established one [13,14]. However, due to a higher density of experimental data, we improve here the accuracy of the diagram (Fig. 3).

Several effects contribute to the specific heat of $NpGa_3$, that can be considered as the sum of the following components:

$$C = C_{ph} + C_{el} + C_{mag} \quad (2)$$

where C_{ph} is the phonon contribution, C_{el} is the electronic part and C_{mag} the magnetic specific heat.

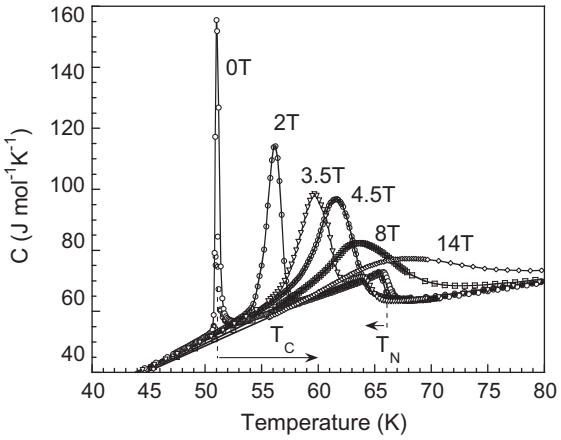

Fig. 2. Specific heat of $NpGa_3$ in applied magnetic fields up to 14 T.

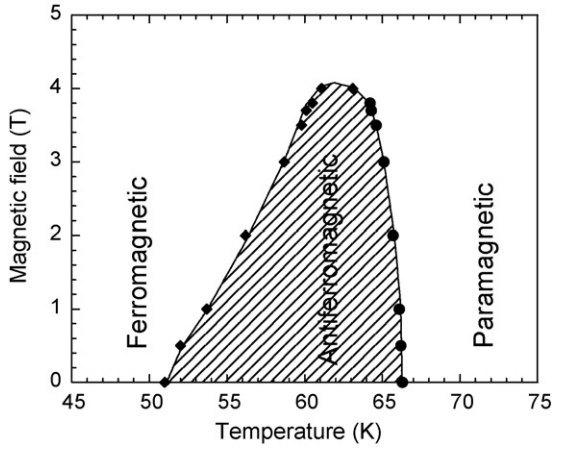

Fig. 3. Magnetic phase diagram of $NpGa_3$ precisely re-built from specific heat data.

At low temperatures, the phonon part can be approximated by a T^3 law and we obtain:

$$C_{el} + C_{ph} = \gamma T + \beta T^3 \quad (3)$$

Below 5 K, we notice an increase of the C/T value (Fig. 4), which indicates the presence of another contribution to the specific heat,

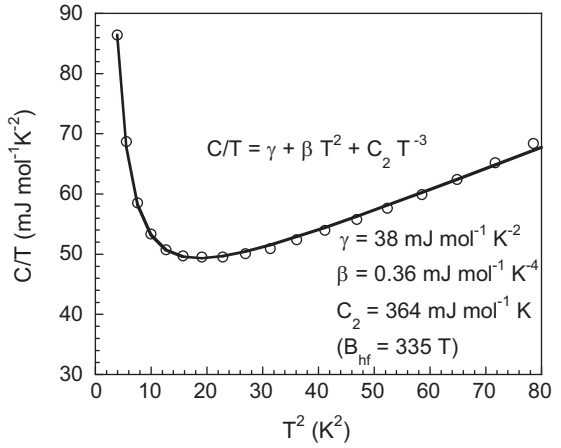

Fig. 4. Low-temperature specific heat of $NpGa_3$. The experimental data (open circles) of C/T are reproduced assuming a constant electronic term, a quadratic temperature dependence of the phonon contribution and a nuclear Schottky anomaly (solid line, see text).

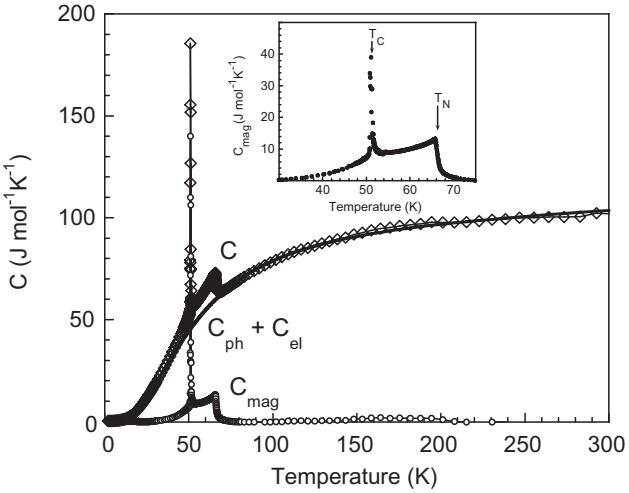

Fig. 5. Total (diamonds), phonon and electronic (solid line) and magnetic (circles) contributions to the specific heat of $NpGa_3$. The inset shows the magnetic specific heat.

ascribed to a nuclear hyperfine Schottky term due to the splitting of the nuclear ground state level ($I = 5/2$) of the ^{237}Np nuclei by the hyperfine field:

$$C_N = \frac{R/3(\mu B_{hf}/k_B I)2I(I+1)}{T^2} = C_2 T^{-2} \quad (4)$$

with R the molar gas constant, k_B the Boltzmann constant, μ the nuclear moment of the ^{237}Np ground state ($2.5\mu_N$), I the nuclear spin of the ^{237}Np ground state (5/2) and B_{hf} the hyperfine magnetic field measured by Mössbauer spectroscopy ($B_{hf} = 335$ T [14]).

Fig. 4 shows the dependence of C/T vs. T^2 below 80 K^2 ($T \sim 9$ K) and a fit involving the electronic, phonon and nuclear terms described above. The magnetic term may also contribute to the specific heat in this temperature region but is estimated to less than 3 mJ mol^{-1} K^{-1} below 10 K (around 1 mJ mol^{-1} K^{-1} at 5 K, using a simple $T^{3/2}$ dependence). Moreover, it would influence mainly the slope of the observed dependence. We cannot thus relate the β obtained from the fit exclusively to phonons, but the γ coefficient characterizing the electronic contribution can be estimated with reasonable precision to $\gamma = 38(4)$ mJ mol^{-1} K^{-2}.

The global magnetic contribution to the specific heat can be extracted from the data by subtracting the other components. The nuclear and electronic specific heat have been estimated from the low-temperature region. The general phonon contribution can be well estimated by a fit of the non-magnetic region using 3 acoustic branches (Debye model, first term) and 6 optic branches (Einstein model, second term):

$$C_{ph} = 9R\left(\frac{T}{\theta_D}\right)^3 \int_0^{\theta_D/T} \frac{x^4 e^x}{(e^x-1)^2} dx + R\sum_{i=1}^{6}\left(\frac{\theta_{Ei}}{T}\right)^2 \frac{e^{\theta_{Ei}/T}}{(e^{\theta_{Ei}/T}-1)^2} \quad (5)$$

With R the gas constant, θ_D and θ_E the Debye and Einstein temperatures, $x = E/k_B T$.

The main contributions to the specific heat of $NpGa_3$ are plotted in Fig. 5. The inset shows the magnetic component around the transitions. It can be observed that the magnetic specific heat contributes significantly between 30 and 70 K.

By integrating the magnetic specific heat, we obtain the magnetic entropy, which is shown in Fig. 6:

$$S_{mag} = \int_0^T C_{mag}(T)\frac{dT}{T} \quad (6)$$

A discontinuity is observed at T_C, where the first-order transition takes place. The magnetic entropy is close to Rln2, suggesting the occurrence of a doublet ground state ($J = 1/2$) and a rather localized system. In comparison, the magnetic entropy at T_N of the itinerant antiferromagnet UGa_3 is barely 0.14 Rln2 [16].

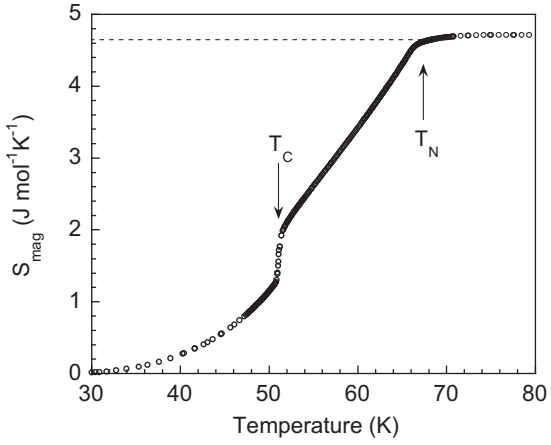

Fig. 6. Magnetic entropy of $NpGa_3$. The value at the onset of magnetic ordering is indicated by a dotted line.

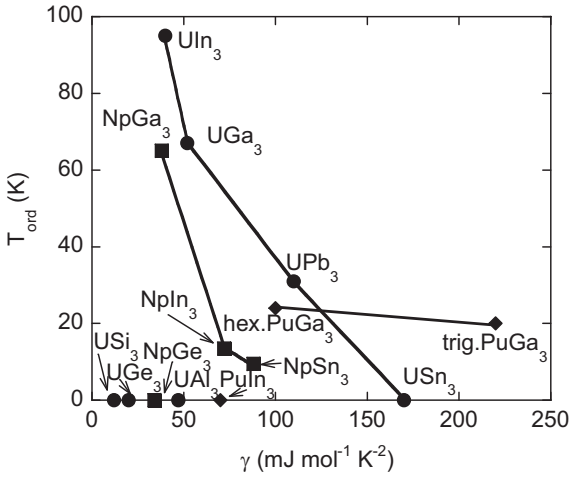

Fig. 7. Ordering temperature plotted as a function of the Sommerfeld specific heat coefficient in AnX_3 compounds (circles for U, squares for Np and diamonds for Pu).

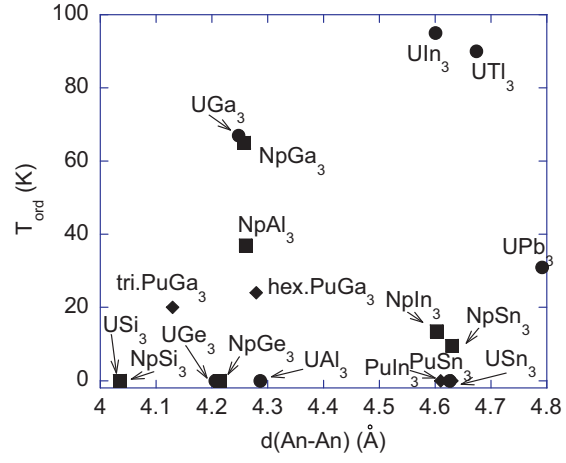

Fig. 8. Hill plot of the AnX_3 compounds (circles for U, squares for Np and diamonds for Pu).

4. Discussion

The analogue compound UGa_3 has a Néel temperature (T_N = 67 K) very close to that of $NpGa_3$ (T_N = 66.5 K) and shares the same type II antiferromagnetic structure (wave vector k = (1/2 1/2 1/2)) [17]. These remarkable similarities contrast with marked differences: in UGa_3 two anomalies are observed by magnetization, resistivity, thermopower and neutron diffraction around 40 K and 10 K, but their nature still remains unexplained [18,19]. An itinerant nature of the *5f*-electron antiferromagnetism has been assigned to UGa_3 on the basis of magnetic and specific heat data (reduced ordered magnetic moment ($0.8\mu_B$), enhanced electronic specific heat coefficient (50 mJ mol^{-1} K^{-2})), strongly reduced magnetic entropy (0.14 Rln2) [16], behavior under high pressure [20,21] and confirmed by further experimental data and band structure calculations [2].

Unlike $NpGa_3$ where the application of pressure reinforces the magnetic coupling and increases the Néel temperature up to 200 K at 15 GPa [15], UGa_3 experiences a rapid collapse of T_N that vanishes around p_c = 2.6 GPa [21]. The latter could be close to a quantum critical point since non-Fermi liquid behavior is observed around p_c, whereas a Fermi liquid regime appears at higher pressures. Furthermore, at 1.5 GPa, the resistivity of UGa_3 starts to drop below 0.3 K and could be indicative of superconductivity [21].

The $PuGa_3$ analogue crystallizes in either a trigonal structure type ($R-3m$) or in the hexagonal DO19 type ($P6_3/mmc$). Both phases order magnetically; the trigonal modification corresponds to a soft ferromagnet below T_C = 20 K with a saturated moment of $0.2\mu_B$/Pu whereas the hexagonal one exhibits antiferromagnetic order below T_N = 24 K which undergoes a metamagnetic transition around 6 T [6]. They both exhibit highly enhanced values of the Sommerfeld coefficient of 110 mJ mol^{-1} K^{-2} and 220 mJ mol^{-1} K^{-2}, respectively. Under high pressure, the Néel temperature of the trigonal $PuGa_3$ [6] increases, similarly to $NpGa_3$ [12] or the parent compound $NpCoGa_5$ [22], whereas the hexagonal modification behaves like UGa_3 [21] with a collapse of T_N.

Fig. 7 shows the variation of the ordering temperature as a function of the specific heat γ coefficient for the whole AnX_3 series. In the uranium and neptunium series, it appears clearly that the ordering temperature collapses with increasing γ, suggesting that the *5f–spd* hybridization and concomitant *5f* delocalization increase from the rather localized $NpGa_3$ to the weak antiferromagnet $NpSn_3$ ($\mu_{Np} = 0.3\mu_B$) or from the antiferromagnet UIn_3 to the paramagnet USn_3. The compounds with the lowest γ are paramagnetic. The trend is less clear in the PuX_3 series, but it should be noticed that only 2 (non-cubic) modifications of the same system ($PuGa_3$) are available.

Although the An–An distance is far beyond the limit of *5f–5f* orbitals overlap (3.2–3.4 Å) in the AnX_3 compounds, it is interesting to look at a Hill plot (Fig. 8) to summarize the situation and observe some trends across the series. First we again notice the similarity between $NpGa_3$ and UGa_3 with identical ordering temperature and close γ values. The Si and Ge samples exhibit the lowest lattice parameters of the series and are paramagnetic. Clearly, UGa_3 is the only uranium-based compound with "short" lattice parameter that orders magnetically. This obviously suggests a strong *5f*–ligand hybridization and explains the itinerant character of this magnet. UAl_3 is a paramagnet whereas $NpAl_3$ orders magnetically. This is consistent with the general trend that neptunium compounds are more localized than uranium analogues, due to the smaller spatial extent of Np *5f* orbitals compared to U. However, the trend is somehow contradicted by UIn_3 that has the highest ordering temperature (T_N = 88 K) of the AnX_3 series and $NpIn_3$ that has one of the lowest (T_C = 13.5 K). Competing interactions (resulting in its complex magnetic phase diagram and magnetic structure) may explain the low ordering temperature of $NpIn_3$ [23].

5. Conclusion

The specific heat of $NpGa_3$ has been investigated for the first time. The magnetic phase transitions have been better characterized and the magnetic phase diagram has been rebuilt more precisely. The moderately enhanced Sommerfeld coefficient and the magnetic entropy close to Rln2 point to a rather localized system, which is consistent with previous studies, in particular high pressure Mössbauer spectroscopy and high pressure electrical resistivity. The comparison with other NpX_3 suggests that $NpGa_3$ is the most localized member of the series. Whereas UGa_3 and hexagonal $PuGa_3$ behave like itinerant systems, $NpGa_3$, trigonal $PuGa_3$ and $NpCoGa_5$ appear as rather localized systems.

Acknowledgements

The authors are grateful to J.P. Sanchez and Y. Haga for fruitful discussions. The high-purity Np metal required for the fabrication of $NpGa_3$ was made available in the framework of a collaboration with the Lawrence Livermore and Los Alamos National Laboratories and the U.S. Department of Energy.

References

[1] D.D. Koelling, B.D. Dunlap, G.W. Crabtree, Phys. Rev. B 31 (1985) 4966–4971.
[2] A.L. Cornelius, A.J. Arko, J.L. Sarrao, J.D. Thompson, M.F. Hundley, C.H. Booth, N. Harrison, P.M. Oppeneer, Phys. Rev. B 59 (1999) 14473–14483.
[3] J. Gal, I. Yaar, S. Fredo, I. Halevy, W. Potzel, S. Zwirner, G.M. Kalvius, Phys. Rev. B 46 (1992) 5351–5356.
[4] J.P. Sanchez, M.N. Bouillet, E. Colineau, A. Blaise, M. Amanowicz, P. Burlet, J.M. Fournier, Physica B 186–188 (1993) 675–677.
[5] J.P. Sanchez, E. Colineau, P. Vulliet, K. Tomala, J. Alloys Compd. 275–277 (1998) 154–160.
[6] P. Boulet, E. Colineau, F. Wastin, P. Javorský, J.C. Griveau, J. Rebizant, G.R. Stewart, E.D. Bauer, Phys. Rev. B 72 (2005) 0644381–0644388.
[7] Y. Haga, D. Aoki, H. Yamagami, T.D. Matsuda, K. Nakajima, Y. Arai, E. Yamamoto, A. Nakamura, Y. Homma, Y. Shiokawa, Y. Ōnuki, J. Alloys Compd. 444–445 (2007) 114–118.
[8] O. Eriksson, B. Johansson, M.S.S. Brooks, H.L. Skriver, Phys. Rev. B 40 (1989) 9508–9518.
[9] V. Sechovsky, L. Havela, in: E.P. Wohlfarth, K.H.J. Buschow (Eds.), Ferromagnetic Materials, vol. 4, Elsevier, 1988, pp. 382–383.
[10] R.J. Trainor, M.B. Brodsky, B.D. Dunlap, G.K. Shenoy, Phys. Rev. Lett. 37 (1976) 1511–1514.
[11] D. Aoki, Y. Homma, H. Sakai, S. Ikeda, Y. Shiokawa, E. Yamamoto, A. Nakamura, Y. Haga, R. Settai, Y. Ōnuki, J. Phys. Soc. Jpn. 75 (2006) 084710–084719.
[12] D. Aoki, H. Yamagami, Y. Homma, Y. Shiokawa, E. Yamamoto, A. Nakamura, Y. Haga, R. Settai, Y. Ōnuki, J. Phys. Soc. Jpn. 74 (2005) 2149–2152.
[13] E. Colineau, F. Bourdarot, P. Burlet, J.P. Sanchez, J. Larroque, Physica B 230–232 (1997) 773–775.
[14] M.N. Bouillet, T. Charvolin, A. Blaise, P. Burlet, J.M. Fournier, J. Larroque, J.P. Sanchez, J. Magn. Magn. Mater. 125 (1993) 113–119.
[15] S. Zwirner, V. Ichas, D. Braithwaite, J.C. Warenborgh, S. Heathman, W. Potzel, G.M. Kalvius, J.C. Spirlet, J. Rebizant, Phys. Rev. B 54 (1996) 12283–12293.
[16] D. Kaczorowski, R. Troć, D. Badurski, A. Böhm, L. Shlyk, F. Steglich, Phys. Rev. B 48 (1993) 16425–16431.
[17] P. Dervenagas, D. Kaczorowski, F. Bourdarot, P. Burlet, A. Czopnik, G.H. Lander, Physica B 269 (1999) 368–372.
[18] D. Aoki, N. Suzuki, K. Miyake, Y. Inada, R. Settai, K. Sugiyama, E. Yamamoto, Y. Haga, Y. Ōnuki, T. Inoue, K. Kindo, H. Sugawara, H. Sato, H. Yamagami, J. Phys. Soc. Jpn. 70 (2001) 538–546.
[19] D. Kaczorowski, J. Phys. Soc. Jpn. 75 (2006) 68–73.
[20] D. Kaczorowski, R. Hauser, A. Czopnik, Physica B 230–232 (1997) 35–38.
[21] M. Nakashima, Y. Haga, F. Honda, T. Eto, G. Oomi, T. Kagayama, N. Takeshita, T. Nakanishi, N. Môri, D. Aoki, R. Settai, Y. Ōnuki, J. Phys. Condens. Matter 13 (2001) L569–L576.
[22] E. Colineau, P. Javorsky′, P. Boulet, F. Wastin, J.C. Griveau, J. Rebizant, J.P. Sanchez, G.R. Stewart, Phys. Rev. B 69 (2004) 1844111–1844118.
[23] E. Colineau, A. Blaise, P. Burlet, J.P. Sanchez, J. Larroque, Physica B 206–207 (1995) 528–530.